15th Canadian Masonry Symposium
Ottawa, Canada
June 2-5, 2025

Identification of Wall Tie Deterioration using Finite Element Model Updating Method

Chee Yin Lam[i], Mark J. Masia[ii], Igor A. Chaves[iii], and Md Akhtar Hossain[iv]

ABSTRACT

Wall tie deterioration in masonry veneer and cavity wall systems is a critical issue that affects the structural reliability of many existing masonry structures. Destructive means are often used to assess the condition of ties, and this can be uneconomical and cause disruption to building use. A non-destructive, vibration-based method was utilized in this study to collect vibration measurements of a masonry veneer wall in its undamaged state along with four different wall tie deterioration cases. For damage identification purposes, a finite element model of the experimentally tested veneer wall was first constructed, and the updating process was then performed to optimize critical material properties that best simulate the experimentally recorded behaviour of the undamaged veneer wall. Utilizing the calibrated reference state model, sample points with varying Young's moduli of wall ties at different locations were strategically selected using the design of experiments methodology to generate an appropriate response surface polynomial model for each of the six natural frequencies. The simplified polynomial models replaced the complex model in the finite element analysis software and were further utilized in the optimization process. The optimization of the Young's moduli of wall ties was then performed to minimize the difference between the experimental and simulated natural frequencies. This finite element model updating approach showed promising performance in terms of condition assessment of wall ties, where the damaged states were reflected by the optimized Young's moduli of wall ties.

KEYWORDS

finite element model updating, masonry, optimization, response surface model, wall tie

[i] Ph.D. Student, The University of Newcastle, Callaghan, Australia, cheeyin.lam@uon.edu.au
[ii] Professor, The University of Newcastle, Callaghan, Australia, mark.masia@newcastle.edu.au
[iii] Associate Professor, The University of Newcastle, Callaghan, Australia, igor.chaves@newcastle.edu.au
[iv] Research Associate, The University of Newcastle, Callaghan, Australia, akhtar.a.hossain@newcastle.edu.au

INTRODUCTION

Wall ties are critical to the construction of multi-leaf masonry structures such as masonry veneer and cavity walls. The connection between the outer brick wall and the inner load-bearing structural element is provided by the wall ties and allows for the transfer of horizontal loads. Since the wall ties are concealed within the cavity of the multi-leaf masonry structures, the condition of wall ties is challenging to assess, and deteriorated wall ties may cause the collapse of the outer brick wall. One of the major concerns of wall tie deterioration is related to the corrosion of wall ties as shown in Figure 1. Many researchers have identified that the portion of the wall tie that is at and within the mortar joint of the outer brick wall suffered a higher degree of corrosion [1-3]. This phenomenon is difficult to identify using conventional wall tie inspection techniques such as borescope, thermal imaging and radar methods [4]. In this case, the removal of bricks may be needed but unfortunately the process is destructive and may further compromise the structural integrity of the existing multi-leaf masonry structures.

Figure 1: Deterioration of wall tie within a masonry cavity wall [2].

One of the promising non-destructive approaches for the condition assessment of wall ties within multi-leaf masonry structures is the use of vibration-based techniques, where the structure is excited using a wide range of vibration sources and the corresponding responses are recorded. Vibration-based techniques have been investigated extensively in terms of damage identification of civil structures, and structural defects were successfully detected based on the vibration measurements [5]. In particular, the natural frequencies and the corresponding mode shapes extracted from the vibration measurements are both good indicators for damage detection purposes. In the context of wall tie deterioration within masonry veneer wall, when the out-of-plane stiffness of a masonry veneer wall was impacted by the absence of wall ties, the natural frequencies reduced and large changes in mode shapes were observed near the damage locations [4]. Even though the experimental study concluded that the deteriorated wall ties can be reasonably identified within a one-storey masonry veneer wall, the damage quantification of the severity of wall tie deterioration was not investigated in the previous study [4].

To further improve the damage localization effectiveness and address the damage quantification aspect, this study has been undertaken to estimate the remaining Young's moduli of the wall ties for different wall tie deterioration cases using the FEMU (finite element model updating) approach based on the response surface methodology [6, 7]. Although the finite element model is an essential numerical tool in structural analysis, uncertainties arising from over idealized boundary conditions and oversimplified assumptions of material behaviours may contribute to discrepancies between analytical and experimental results. In order to mitigate the uncertainties, FEMU was first performed to calibrate sensitive material parameters of the initial numerical model. Then, the reference state model was further utilized to identify, locate and quantify the damage extent. The flowchart of the FEMU approach is detailed in Figure 2 and the steps are further elaborated as follows:

1) Vibration measurements of the masonry veneer wall in its undamaged and damaged conditions were first collected, and a preliminary finite element model was built based on material properties obtained from the material characterization tests and existing literature.
2) Material properties that significantly affect the natural frequencies were identified, and response surface models were built based on DOE (design of experiments) to approximate the natural frequencies of the structure without running a huge number of simulations. Optimization of the selected material properties was performed by minimizing the difference between the simulated and experimental baseline natural frequencies, thus forming the reference state model that reflects the physical system accurately.
3) Focusing on the wall tie deterioration phenomena and utilizing the reference state model, Step 2 was repeated, where the identified material properties used in constructing response surface models were replaced by the varying Young's moduli of wall ties at different locations. Damage identification was then achieved by validating the optimized Young's moduli of wall ties with the actual damaged conditions.

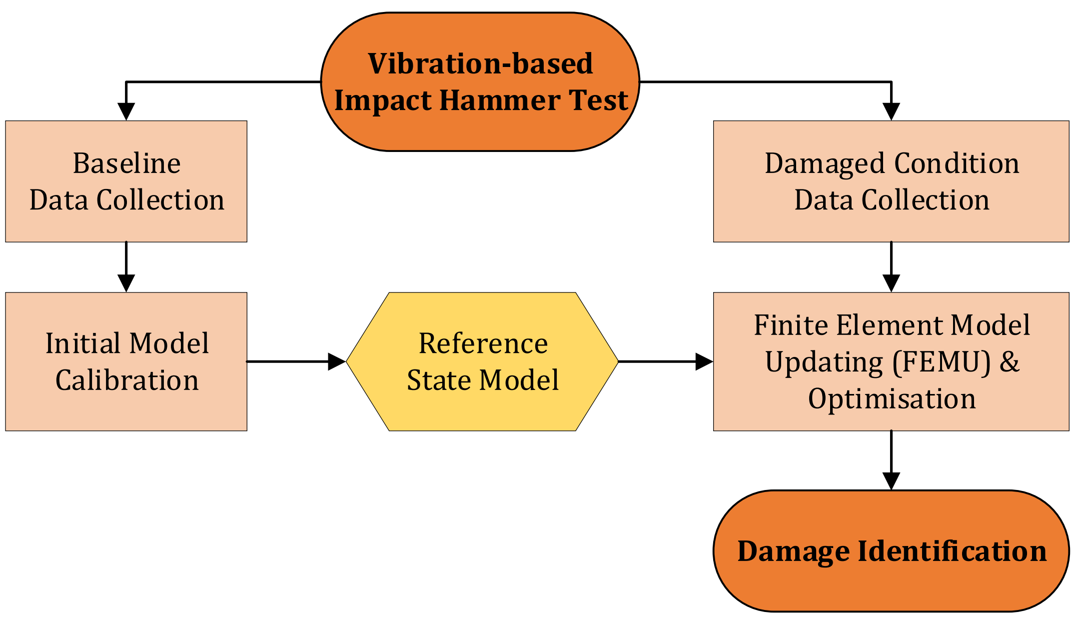

Figure 2: Flowchart of the finite element model updating process.

METHODOLOGY

As outlined in Figure 2, the study involved two aspects, the collection of vibration measurements and the finite element model updating process. In terms of data collection, a one-story masonry veneer wall was built, and an impact hammer was utilized to generate vibrations while the corresponding acceleration responses were recorded using two accelerometers. The dimensions of the masonry veneer wall and the impact hammer testing procedure are shown in Figure 3 and Figure 4 respectively. The top of the timber frame was simply supported, and further details regarding the material specifications can be found in [4].

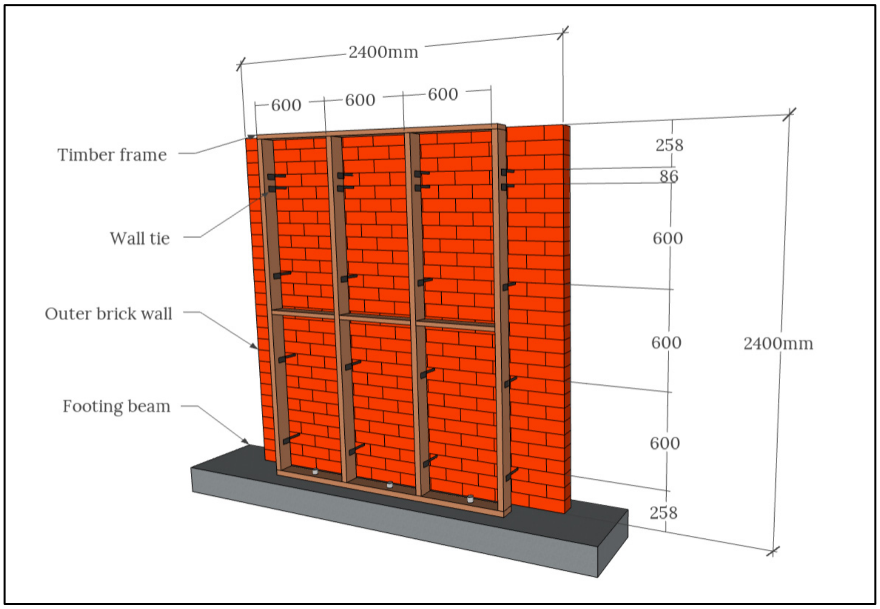

Figure 3: Dimensions of the tested masonry veneer wall.

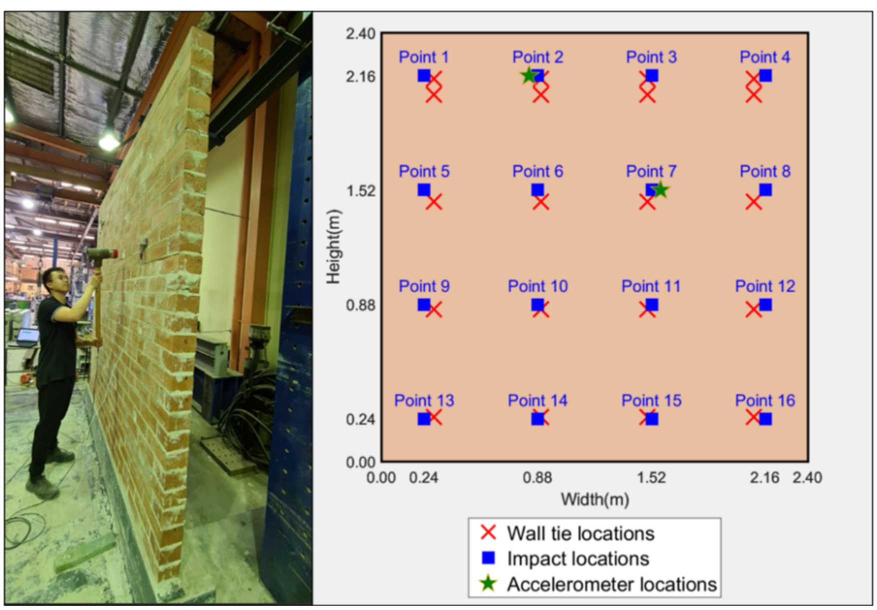

Figure 4: Impact hammer testing procedures.

The impact hammer test was repeated five times to collect vibration measurements for the reference and four different damaged states of the veneer wall respectively. A summary of all the test cases is detailed in Table 1 [4], where attention has been given to identifying deteriorated wall ties at different heights.

Table 1: Summary of the wall tie deterioration cases [4].

Test case	Description of wall tie deterioration
VW1a (Reference)	All ties are fully functional.
VW1b	Top two rows of wall ties were unscrewed.
VW1c	Middle row of wall ties was unscrewed.
VW1d	Second last row of the wall ties was unscrewed.
VW1e	Bottom row of wall ties was unscrewed.

Masonry Veneer Wall Finite Element Model

According to the physical dimensions of the masonry veneer wall, as shown in Figure 3, an initial base model was constructed based on the simplified micro-modelling strategy in DIANA 10.8 [8]. The brick units and timber studs were modelled as linear elastic elements. The joint and unit-joint interfaces were considered collectively using the combined crack-shear-crush model [8]. As for the wall ties, truss elements were selected with a uniaxial non-linear elastic material property which was defined by the compressive and tensile tests of the veneer wall ties [9]. A detailed summary of all the material properties used in the model can be found in [9] where assumptions have been made for some of the material properties or from existing literature. However, a few material parameters were modified based on the material characterization tests explicitly conducted for the masonry veneer wall tested in the current study. The tests included a masonry compression test, lateral modulus of rupture test, bond wrench test and shear triplet test in accordance with AS 3700:2018, AS/NZS 4456.15:2003 and EN 1052-3 respectively [10-12]. The updated material properties are summarized in Table 2.

Table 2: Updated material properties based on a series of material characterization tests.

Parameter	Value	Material characterization test
Elastic modulus of brick	31338 N/mm^2	Masonry compression test
Direct tensile strength	1.332 N/mm^2	Lateral modulus of rupture test
Linear normal stiffness of mortar joint	231 N/mm^3	Masonry compression test
Linear shear stiffness of mortar joint	96 N/mm^3	Masonry compression test
Tensile strength	0.26 N/mm^2	Bond wrench test
Cohesion (shearing)	0.40 N/mm^2	Shear triplet test
Friction angle (shearing)	0.86 rad	Shear triplet test
Masonry compressive strength (crushing)	12.37 N/mm^2	Masonry compression test
Equivalent plastic relative displacement	0.014 mm	Masonry compression test

Meanwhile, the schematic diagram of the masonry veneer wall finite element model is shown in Figure 5, where the bottom of the timber studs and outer brick wall were pin supported while the top of the timber studs was restrained against translation in the out-of-plane direction.

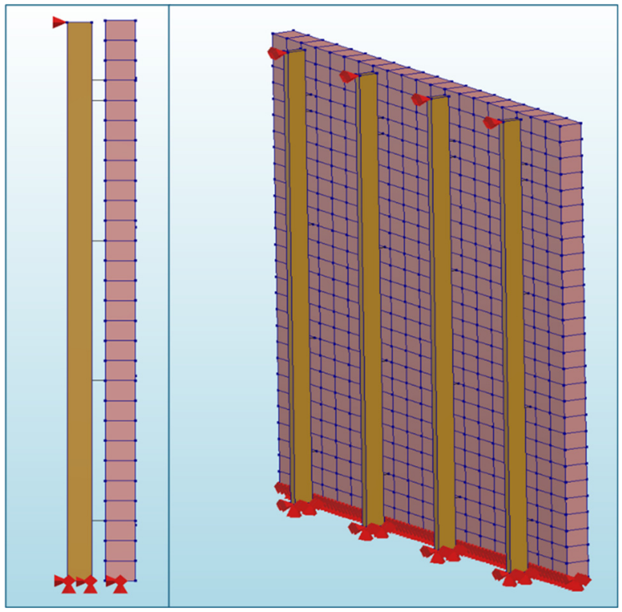

Figure 5: Numerical model of the one-storey masonry veneer wall.

Results and Discussion

Modal analysis was first performed to determine the natural frequencies and the corresponding mode shapes from the vibration measurements. The first six natural frequencies that were obtained consistently from all test cases are summarized in Table 3. The two-stage finite element model updating processes were then carried out subsequently.

Table 3: Six natural frequencies that were obtained from all test cases.

Test case	Natural frequency (Hz)					
	Mode 1	Mode 2	Mode 3	Mode 4	Mode 5	Mode 6
VW1a (Reference)	9.12	20.52	30.54	56.66	131.86	187.06
VW1b	5.64	17.94	28.17	55.58	131.36	186.75
VW1c	8.64	19.79	29.32	55.72	128.51	185.63
VW1d	8.69	19.93	29.52	56.12	130.72	187.31
VW1e	8.68	19.95	29.54	56.09	131.03	186.22

Finite Element Model Updating

Initial model calibration

Firstly, the initial model calibration was conducted to establish the reference state model by minimizing the difference between the simulated and experimental natural frequencies from the reference state. By conducting a sensitivity analysis, a total of four parameters were found to be influential on the natural frequencies of the initial veneer wall model. These parameters were the normal stiffness modulus of unit-mortar interface (k_n), Young's moduli of timber (E_{timber}), wall tie (E_{wt}) and brick (E_{brick}) respectively. The identified material properties were all obtained from material characterization tests, where the mean values and their corresponding standard deviations are presented in Table 4.

Table 4: Sensitive material properties that influence the initial veneer wall model.

	k_n	E_{timber}	E_{wt}	E_{brick}
Mean value	231 N/mm^3	11378 MPa	6044 MPa	31338 MPa
Standard deviation	55 N/mm^3	1892 MPa	1179 MPa	5026 MPa

The DOE approach, in particular the central composite design approach (CCD) [6] was employed by exploring the selected material properties within three standard deviations away from the mean values, resulting in 36 DOE cases. After running the simulations for each DOE case, six polynomial response surface models were formed, where each polynomial equation corresponded to one of the six measured natural frequencies. The main idea is to eliminate the time-consuming process of conducting full finite element analysis after each iteration in the optimization process. Instead, the natural frequencies can be directly estimated using the less complex polynomial functions.

Quadratic polynomials were deemed sufficient for the six response surface models, as justified by high adjusted R^2 values with an averaged value of 0.9905. To further justify the selection of the sensitive parameters, the parameter significance of all sensitive material properties in all six response surface models was investigated where p-values lesser than 0.05 indicate that the parameter significantly affects the natural frequencies. The p-values of the selected material properties were less than 0.05 for the first three modes, but the Young's moduli of timber and wall tie showed a higher value for the remaining modes. Since the higher modes may exhibit more variability due to noise in the experimental data, the p-values higher than 0.05 may not indicate low significance of the parameter. Instead, it could reflect the decreased reliability of the data. Hence, the selected four material properties were still included in the analysis.

The optimization algorithm used in the study is '*fmincon*' in MATLAB [13] and the objective function (ε) to be minimized is shown in Eq. (1), where m is the number of vibration modes, ω_{sim} and ω_{exp} are the simulated and experimental natural frequencies respectively.

$$(1) \quad \varepsilon = \sum_{i=1}^{m} \left(\frac{\omega_{i,sim} - \omega_{i,exp}}{\omega_{i,exp}} \right)^2$$

By minimizing the objective function, the optimized k_n, E_{timber}, E_{wt} and E_{brick} were obtained as 122N/mm^3, 7208 MPa, 9581 MPa and 18107 MPa respectively, forming the basis of the reference state model. The averaged percentage error of the natural frequencies decreased from 30.67% to 5.82%, indicating that the reference state model is more representative of the experimentally tested veneer wall compared to the initial numerical model. Comparisons of the initial and the reference state models are presented in Figure 6.

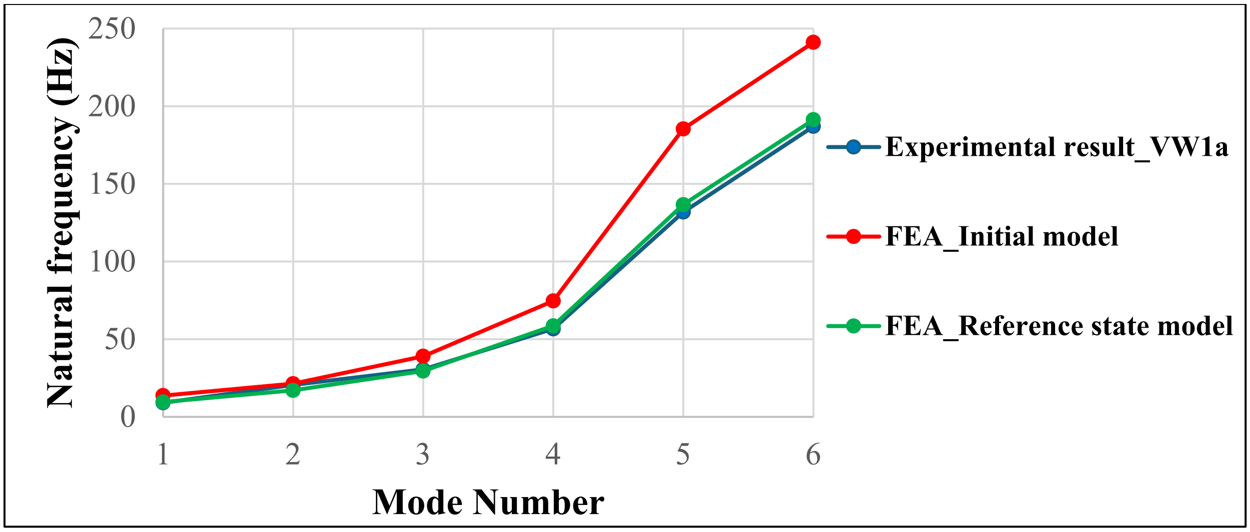

Figure 6: Comparisons of the natural frequencies obtained before and after the optimization process.

Damage identification

Following a similar approach for calibrating the reference state model, the damage identification process was carried out by optimizing the Young's moduli of the wall ties at four different heights to reflect the absence of wall ties. Instead of optimizing the Young's modulus of each individual wall tie, wall ties in the same row were grouped together and treated as one parameter to avoid a huge number of DOE cases when forming the response surface models. The decision was further justified by the load-sharing behaviour of veneer wall ties during out-of-plane loading conditions where the wall ties in the same row shared a similar amount of load [9]. Therefore, the four parameters to be optimized are E_{wt13_20} (top two rows), E_{wt9_12} (middle row), E_{wt5_8} (second bottom row) and E_{wt1_4} (bottom row) respectively. Based on the reference state model, the Young's modulus of the undamaged wall tie was estimated as 9581MPa. When damage occurs to the wall ties, it is expected that the Young's modulus of wall tie should reduce accordingly, hence the DOE approach was employed by exploring the Young's moduli of wall ties within a range of 1% to 100% of 9581MPa. When forming the response surface models, more boundary cases were sampled in addition to the conventional central composite design to improve the coverage of parameter space, especially when the actual damaged conditions often correspond to the extremes of the parameter (values close to 1%). This resulted in a total of 72 DOE cases.

In this second stage of FEMU, cubic polynomials were selected as the response surface models which achieved higher adjusted R^2 values with an averaged value of 0.9927 while quadratic polynomials were only able to achieve an averaged value of 0.8905. While the parameter significance for the four selected Young's moduli of wall ties was greater than 0.05 for some modes, indicating that the parameters do not always affect the natural frequencies significantly, the physical relevance of each parameter is critical in terms of the damage identification purposes, hence the parameters were still included in the analysis.

Once the response surface models were constructed for the six natural frequencies, the optimization process was carried out for each damage scenario subsequently by minimizing the difference between the simulated and experimental natural frequencies. The results of the optimized Young's moduli of wall ties at four different locations are presented in Table 5 with values ranging from 0.01 to 1 of 9581MPa. The highlighted green cells represent the actual damage locations, while the values highlighted in red are the lowest value in each test case.

Table 5: Optimized Young's moduli of wall ties for each test case, ranging from 0.01 to 1 of its value obtained from the reference state model.

Test case	Optimized E_{wt} from FEMU			
	E_{wt13_20}	E_{wt9_12}	E_{wt5_8}	E_{wt1_4}
VW1b	0.13	0.91	1.00	0.53
VW1c	0.73	0.01	0.76	1.00
VW1d	0.82	0.25	0.12	1.00
VW1e	0.84	0.39	0.14	0.01

Furthermore, the optimized natural frequencies using the response surface models (ω_{opt}) after the optimization process and the percentage errors ($\Delta\omega$) when compared with the experimental ones are presented in Table 6. The percentage errors are further visualized in Figure 7.

Table 6: Optimized natural frequencies obtained from the FEMU process and the corresponding percentage errors when compared with the experimental natural frequencies.

	VW1b		VW1c		VW1d		VW1e	
	ω_{opt} (Hz)	$\Delta\omega$(%)	ω_{opt} (Hz)	$\Delta\omega$(%)	ω_{opt} (Hz)	$\Delta\omega$(%)	ω_{opt} (Hz)	$\Delta\omega$(%)
Mode 1	5.71	1.19	8.95	3.54	9.03	3.85	9.05	4.29
Mode 2	15.52	13.50	16.62	16.01	16.69	16.27	16.69	16.33
Mode 3	27.98	0.68	29.45	0.42	29.31	0.70	29.20	1.15
Mode 4	58.44	5.15	58.45	4.89	58.52	4.27	58.57	4.42
Mode 5	131.25	0.08	129.99	1.15	131.67	0.73	132.20	0.89
Mode 6	186.68	0.03	187.87	1.21	186.35	0.51	186.95	0.39
	Average	3.44		4.54		4.39		4.58

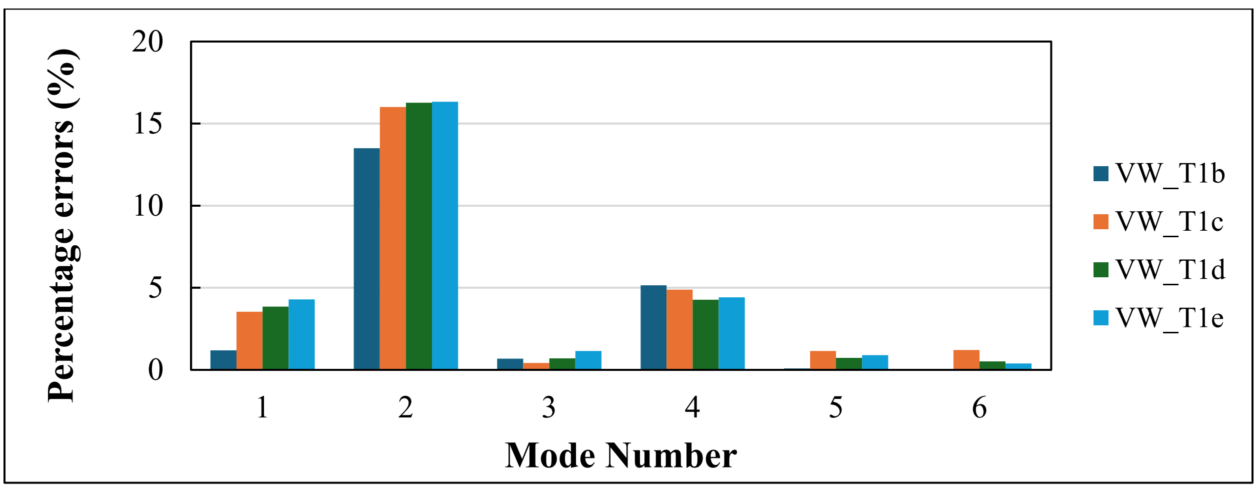

Figure 7: Percentage errors of the optimized and experimental natural frequencies for each test case.

From Table 5, the optimized Young's modulus of wall ties at the actual damage location consistently reached its minimum value for all deterioration test cases, while the Young's moduli of wall ties at the undamaged locations did not always yield a value very close to 1. Potential sources of not achieving exactly 1 at the undamaged locations may include the accuracy of the response surface models, sampling technique for the DOE cases, the convergence of the selected optimizing algorithm and the limitations in the finite element model. The limitation of the numerical model was further evident when the percentage error for the reference state model was obtained as 5.82%, indicating a slight discrepancy when representing the veneer wall in the finite element model. In terms of forming response surface models, the limited number of DOE cases may lead to a less accurate response surface model. Although increasing the number of DOE cases may lead to a more accurate response surface model, striking a balance to save time and computational efforts is equally critical. Nevertheless, the FEMU process demonstrated reasonable accuracy in identifying the deteriorated wall ties despite the minor variations.

From Table 6 and Figure 7, the averaged percentage error between the optimized and experimental natural frequencies for each test case was below 5%. Out of the six vibration modes, the largest discrepancy was Mode 2 across all test cases with an averaged value of 15.5% while most of the remaining optimized natural frequencies matched quite well with the experimental ones. The large discrepancy for Mode 2 may once again be due to limitations of the finite element model where over idealized boundary conditions and certain material model assumptions were considered during the model construction phase.

Another possible source of uncertainty could be the mismatch of geometric properties which was reported in [14] that the dynamic responses were sensitive to the dimensions considered in the masonry arch model. For this study, perfect dimensions for the bricks and mortar joints were considered for the veneer wall finite element model while the mortar thicknesses may vary significantly and highly dependent on the workmanship of the bricklayer.

CONCLUSION

This study investigates the performance of FEMU using the response surface methodology to identify the deteriorated wall ties within a masonry veneer wall. The vibration measurements of the veneer wall in its undamaged and four different damaged conditions were collected from the impact hammer test. A numerical model of the veneer wall was built and calibrated by optimizing sensitive material parameters to achieve the smallest difference between the simulated and experimental natural frequencies. The optimized Young's moduli of wall ties for each damaged condition successfully reflected the actual wall tie damage locations and showed promising results in terms of damage localization, though further research is suggested to improve the damage quantification aspect.

Since the FEMU method relies on the natural frequencies as input, the vibration data quality has a direct influence on the proposed FEMU. Therefore, coherence needs to be checked, and the force level of each impact needs to be kept at a consistent level to ensure consistency. Additionally, factors such as the angle and locations of impact affect the data quality as indicated in [15], hence care must be taken during the impact hammer test.

When comparing FEMU with other vibration-based damage identification methods, the unique advantage is the use of natural frequencies as the sole input whereas other methods require additional mode shape data and its derivatives to locate damage, where mode shape data typically contains more noise compared to natural frequencies. Furthermore, other vibration-based methods are only capable of providing qualitative interpretation of damage locations, but FEMU is capable of further quantifying the damage extent. In terms of the practicality of this method, baseline vibration data is needed to first calibrate the initial finite element model, and it is not always available especially for older or retrofitted structures. However, a good starting point for calibrating the initial model can be achieved by considering available theoretical design specifications, historical information on the test structure and visual inspection.

Future studies are recommended to investigate different types of boundary conditions and material models that could represent the actual behavior of the veneer wall more closely. The effect of increasing the number of DOE cases used when forming the response surface models, utilizing different optimizing algorithms and incorporating the mode shape information in the objective function may be worth exploring to improve the effectiveness of this FEMU approach.

ACKNOWLEDGEMENTS

The financial support provided by The University of Newcastle through the UNIPRS and UNRS Central Scholarships and the Australian Research Council under the Linkage Project - LP220100028 is gratefully acknowledged. The authors would also like to acknowledge the generosity of EngAnalysis for providing the impact hammer and the assistance provided by the civil laboratory staff at The University of Newcastle to setup various testing equipment.

REFERENCES

[1] Chaves, I.A., de Prazer, S., Jardim do Nascimento, B., Flowers, G. (2021). "Empirical coastal atmospheric corrosion of masonry metal wall ties." *Corrosion and Materials Degradation 2*, 657–665.

[2] Page, A.W. (2019). "The Newcastle earthquake and the masonry structures code AS3700." *Proceedings of 2019 AEES conference,* Newcastle, Australia.

[3] Maurenbrecher, A. and Brousseau, R. (1993). *Review of corrosion resistance of metal components in masonry cladding on buildings.* National Research Council Canada, Institute for Research in Construction.

[4] Lam, C.Y., Hossain, M.A., Masia, M.J., Chaves, I.A., Vazey, J. (2024). "Detecting corroded wall ties through non-destructive means." *Corrosion and Prevention 2024*, Cairns, Australia.

[5] Fan, W. and Qiao, P. (2011). "Vibration-based damage identification methods: A review and comparative study." *Structural Health Monitoring,* 10 (2011) 83–111.

[6] Fang, S.E. and Perera, R. (2009). "A response surface methodology based damage identification technique." *Smart Materials and Structures*, 18(6), p.065009.

[7] Ren, W.X. and Chen, H.B. (2010). "Finite element model updating in structural dynamics by using the response surface method." *Engineering structures*, 32(8), pp.2455-2465.

[8] DIANA FEA BV. (2024) DIANA Finite Element Analysis, Release Note 10.8, Delft, The Netherlands.

[9] Muhit, I.B. (2021). "Stochastic Assessment of Unreinforced Masonry Veneer Wall Systems Subjected to Lateral Out-of-Plane Loading." PhD thesis, The University of Newcastle, Australia.

[10] Standards Australia. (2018). *Masonry Structures* (AS 3700:2018). Standards Australia. Sydney, Australia.

[11] Standards Australia. (2003). *Masonry units, segmental pavers and flags-Methods of test Structures* (AS/NZS 4456.15:2003). Standards Australia. Sydney, Australia.

[12] UNI EN. (2002). *Methods of test for masonry. Part 3: Determination of initial shear strength.* (EN 1052-3). Brussels, Belgium.

[13] The MathWorks Inc. (2022). Optimization Toolbox version: 9.4 (R2022b), Natick, Massachusetts: The MathWorks Inc. https://www.mathworks.com

[14] Ramos, L.F. (2007). "Damage identification on masonry structures based on vibration signatures." PhD thesis, University of Minho, Portugal, 2007.

[15] Avitabile, P. (2018). *Modal testing: a practitioner's guide*, John Wiley & Sons, Hoboken, NJ.